Accepted Manuscript

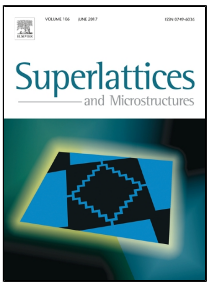

Enhancement in the Efficiency of Crystalline Cu_2ZnSnS_4 Thin Film Solar Cell by using Various Buffer Layers

Sandip Mahajan, Dimitra Sygkridou, Elias Stathatos, Nanasaheb Huse, Alexandros Kalarakis, Ramphal Sharma

PII:	S0749-6036(17)30826-1
DOI:	10.1016/j.spmi.2017.05.009
Reference:	YSPMI 4987
To appear in:	*Superlattices and Microstructures*
Received Date:	04 April 2017
Accepted Date:	03 May 2017

Please cite this article as: Sandip Mahajan, Dimitra Sygkridou, Elias Stathatos, Nanasaheb Huse, Alexandros Kalarakis, Ramphal Sharma, Enhancement in the Efficiency of Crystalline Cu_2ZnSnS_4 Thin Film Solar Cell by using Various Buffer Layers, *Superlattices and Microstructures* (2017), doi: 10.1016/j.spmi.2017.05.009

Research Highlights

- Nanostructured CZTS thin films were prepared by SILAR method.
- Improvement the efficiency of CZTS thin film solar cells using different buffer layers such as CdS, ZnS and $Cd_{7.23}Zn_{2.77}S_{10.}$
- Comparative study of CdS, ZnS and $Cd_{7.23}Zn_{2.77}S_{10}$ buffer layers and its structural, optical, morphological and electrical studies.
- The petals or rod like morphology of $Cd_{7.23}Zn_{2.77}S_{10}$ buffer layer has improved the efficiency is around to be 1.24%.

Enhancement in the Efficiency of Crystalline Cu_2ZnSnS_4 Thin Film Solar Cell by using Various Buffer Layers

Sandip Mahajan[a,b,c], Dimitra Sygkridou[c,d], Elias Stathatos [c]**, Nanasaheb Huse [a], Alexandros Kalarakis[e], Ramphal Sharma[a,b,]*

[a]Thin Film and Nanotechnology Laboratory, Department of Physics, Dr. Babasaheb Ambedkar Marathwada University, Aurangabad-431004, (M.S.), India.

[b]Department of Nanotechnology, Dr. Babasaheb Ambedkar Marathwada University, Aurangabad-431004, (M.S.), India.

[c]Nanotechnology & Advanced Material Laboratory, Department of Electrical Engineering, Technological-Educational Institute of Western Greece, GR-263 34, Greece.

[d]Physics Department, University of Patras, GR-265 00, Greece.

[e] Department of Mechanical Engineering, Technological-Educational Institute of Western Greece, GR-263 34, Greece.

*Corresponding author: Prof. Dr. Ramphal Sharma (ramphalsharma@yahoo.com)

Telephone: +91-9422793173, +91-240-2401365/240-2403284; Fax: +91-240-2403115/2403335

**Co-Corresponding author: Prof. Dr. Elias Stathatos (estathatos@teiwest.gr), Telephone/Fax: +30-2610-369242.

Abstract

The incorporation of different types of buffer layers has demonstrated to improve the efficiency of Cu_2ZnSnS_4 (CZTS) thin film solar cells. The materials tested as buffer layers were Cadmium Sulphide (CdS), Zinc Sulphide (ZnS) and Cadmium Zinc Sulphide ($Cd_{7.23}Zn_{2.77}S_{10}$). The effect of the buffer layer and the absorber layers on the structural, morphological and optical properties of the films was studied. As grown CZTS thin films made with SILAR method were annealed at 550 °C in the sulfur atmosphere for 60 min to improve the crystallinity of the material. X-ray diffraction (XRD) and Raman studies confirm the formation of kesterite structure in CZTS thin film. CdS, ZnS and $Cd_{7.23}Zn_{2.77}S_{10}$ thin films also confirm crystalline nature with crystallite sizes being 9 nm, 13 nm and 14 nm respectively. Leaf, flower and petal−like morphologies of CdS, ZnS and $Cd_{7.23}Zn_{2.77}S_{10}$ thin films respectively have been confirmed by Field Emission Scanning Electron Microscopy (FESEM). The electrical properties of the completed CZTS solar cells were also examined. From the obtained J-V characteristic curves upon illumination of the heterojunction solar cells, we calculated the power conversion efficiency to be 0.76 %, 1.00 % and 1.24 % for the FTO/ZnO/ZnS/CZTS/Ag, FTO/ZnO/CdS/CZTS/Ag and FTO/ZnO/ $Cd_{7.23}Zn_{2.77}S_{10}$/CZTS/Ag respectively.

Keywords: Buffer layers, Morphologies, Leaf−like, Flower−like, Petal−like, Efficiency.

1. Introduction

Cu_2ZnSnS_4 (CZTS) is one of an ideal materials for photovoltaic applications due to its high absorption coefficient (10^4 cm^{-1}), optimum direct band gap 1.45 eV for heterojunction solar cells which also matches with solar spectrum and maximum theoretical efficiency 32.4 %. CZTS is earth abundant, non toxic, easily producible and inexpensive material compared to CIGS, CIS and Silicon solar cells [1-4]. The highest laboratory efficiency of CZTS 9.5% and CZTSSe 12.6% were recorded for CdS/CZTS and CdS/CZTSSe heterojunction solar cells [5, 6]. This type of heterojunction solar cells has low power conversion efficiency compared to CIGS solar cell because of the small grain size and the high series resistance of junction. Researchers are focusing on improving the efficiency by using different buffer layers [7]. There are several methods for preparing CZTS thin films via physical and chemical methods [8, 9]. However, Successive Ionic Layer Adsorption and Reaction (SILAR) method is very cheap to easily produce and synthesize CZTS thin film at room temperature [10]. A buffer layer can attain the continuous charge carrier transport such as electrons, which is a major advantage for the heterojunction solar cells. Usually, in heterojunction solar cells, the charge carriers have to cover a long distance from the absorber layer to the buffer layer. As a result, a low resistance buffer layer is very important in order to improve the efficiency and decrease the series resistance [11]. Some suitable buffer layers commonly used in heterojunction solar cells include ZnO, ZnS, CdS, ZnMgO, SnS_2, In_2S_3, and $Cd_{1-x}Zn_xS$ [7, 12]. The nanostructured CdS can be used as a buffer layer material in solar cells because of its high absorption coefficient and wide energy band gap (2.42eV) [13]. ZnS also has a wide energy band gap (3.8 eV), which is an indication of a high optical transmission in the visible region. ZnS has also been used as a non-toxic and relatively inexpensive material in solar cells [14]. Window layer has been used for minimizing the

interface recombination losses and for improving the large band bending. A recent development with a high potential ternary material is $Cd_{1-x}Zn_xS$ thin film, which is even less toxic and more efficient as a buffer material [15]. The ZnO thin film was prepared by Chemical Bath Deposition (CBD) method on glass substrates [16]. Nanostructured CdS, ZnS and $Cd_{1-x}Zn_xS$ thin films were also prepared by the CBD method at 80 °C. The use of the CBD method ensures controlled buffer layers' thickness and highly efficient heterojunction solar cells [17].

In this paper, we report the fabrication of CZTS heterojunction solar cells with different buffer layers. The structural properties of all films were examined by XRD and Raman techniques while their optical properties, such as the absorbance and the band gap estimation were studied by UV-Vis spectrophotometer. Their surface morphology was analyzed by FESEM images and the electrical properties of the cells were studied by the J-V characteristic curves. In particular, ZnO/CdS/CZTS, ZnO/ZnS/CZTS and ZnO/$Cd_{1-x}Zn_xS$/CZTS solar cells were manufactured on fluorine doped tin oxide (FTO) glass substrates and their power conversion efficiency (PCE) is measured.

2. Experimental

Nanostructured CZTS thin films were prepared by the SILAR method at room temperature on glass substrates. For the synthesis we used $CuSO_4.5H_2O$ as a source for Cu, $ZnSO_4.7H_2O$ for Zn, $SnCl_2.2H_2O$ for Sn, and Na_2S for S. Ammonia was used to maintain the pH and control the precipitation of the reaction [18]. After the preparation of the CZTS thin films, they were annealed under an H_2S atmosphere at 550 °C for 60 min to improve the crystallinity of the material [19]. The nanostructured CdS thin film was deposited on glass substrates by CBD. The bath solution consisted of 1M cadmium sulfate ($CdSO_4$) as a source for cadmium, 1.2M thiourea

($SC(NH_2)_2$) as a source for sulfide and 11M ammonium hydroxide (NH_4OH) to maintain the pH of the solution [[13]. The nanostructured ZnS thin film was prepared by soft chemical procedures on silica glass substrates. Soft chemical methods are low cost techniques, requiring simple instrumentation and are suitable for large production [17]. In this experiment, an aqueous solution of 0.1 Zinc Sulphate ($ZnSO_4.H_2O$) and 0.2M thiourea were separately prepared. Then, a few drops of ammonia were added in both solutions with constant magnetic steering for a few minutes and consequently the two solutions were mixed together [14]. The $Cd_{1-x}Zn_xS$ thin film was also deposited on glass substrates and the chemicals used were 0.08 M cadmium sulphate, 0.02M zinc sulphate and 0.2M thiourea. The temperature was increased slowly up to 80 °C during the nucleation process while the ammonium hydroxide was kept constant [15]. All CdS, ZnS and $Cd_{1-x}Zn_xS$ solutions were kept at 80 °C for 60 min to complete the deposition on the glass substrates. ZnO thin films were prepared by chemical bath deposition on a glass substrate at 60 °C for 60 minutes. We used Zinc chloride as a source for Zn, distilled water (H_2O) as a source of O and ammonia for controlling the precipitation and maintaining the pH of the solution [16].

2.1 Solar cell fabrication

For the fabrication of the solar cells, the films were deposited either on Fluorine doped Tin Oxide (FTO, sheet resistance 8 Ω/sq., Pilkington) glass substrates. We designed three different buffer layers configurations solar cells, i.e. FTO/ZnO/ZnS/CZTS, FTO/ZnO/CdS/CZTS and FTO/ZnO/$Cd_{1-x}Zn_xS$/CZTS. The current-voltage (J-V) characteristics of the devices were recorded by using a Keithley Source Meter (model 2601A) under dark and illumination. Finally, a comparison of the three different solar cell configurations (FTO/ZnO/ZnS/CZTS, FTO/ZnO/CdS/CZTS and FTO/ZnO/$Cd_{1-x}Zn_xS$/CZTS) was carried out.

2.2 Material characterization

The Field Emission Scanning Electron Microscope (FESEM) images were obtained from S-4800(HI-9276-0010) under 3keV accelerating voltage for determining the surface morphology of the materials. The phase identification and the crystallite size were measured by Bruker AXS, Germany (D8 Advanced). X-ray Diffraction patterns were obtained in a scanning range 20^o-80^o (2θ) using CuKα_1 radiation with wavelength 1.5406 Å. The Raman spectra were collected by an HR 800 micro-Raman system (JY), using the 633 nm excitation wavelength emitted from a HeCd laser with a scanning range of 100 to 800 cm^{-1}.The optical absorption studies were performed using Perkin Elmer spectrophotometer (Perkin Elmer Lambda-25 UV-Vis Spectrophotometer) in the range 400-1100 nm wavelength. A solar simulator (Solar Light 16S−300) with a Xenon lamp was used to illuminate the cells where the irradiation was adjusted to100 mW/cm^2. The electrical data of the CZTS solar cells were studied by the current–voltage (J–V) characteristics [Keithley Source Meter (model 2601A)] which were recorded using computer software (LabTracer).

3. Results and Discussion

3.1 Structural properties

The structural analysis of CZTS, ZnO, CdS, ZnS and $Cd_{7.23}Zn_{2.77}S_{10}$ thin films were carried out by using X-ray diffractometer (XRD) instrument. Figure 1(a) shows the XRD pattern of CZTS thin film on glass substrate. The peaks of 2θ values at 28.53^o, 47.32^o, 56.17^o and 64.18^o are due to the reflections from the kesterite planes of CZTS (1 1 2), (2 2 0), (3 1 2) and (3 1 4) respectively (JCPDS No. 26-0575) [18]. These results revealed that the CZTS thin films prepared by the SILAR method have a polycrystalline structure. Figure 1(b) indicates the Raman

scattering spectra of CZTS thin film. A sharp peak at 339cm^{-1} and a broader peak at 286cm^{-1} are observed, which can be assigned to pure CZTS without any additional peaks of other binary or ternary sulfides [20]. Larger grains' size and pure polycrystalline structure of CZTS thin film can improve the efficiency of the corresponding heterojunction solar cells [21]. The nanocrystalline structure of the ZnO thin films was confirmed by the XRD pattern shown in Figure 1(c). ZnO thin films have hexagonal structure with the orientation of (1 0 0), (0 0 2), (1 0 1), (1 0 2) and (1 0 3) planes [22]. The structural parameters of CZTS and ZnO thin films shown in table 1. The XRD pattern of the CdS thin films which were deposited by the CBD method is shown in Figure 2(a). The results indicate that the obtained CdS thin films have the cubic structure of 2θ values at 26.54^{o} and 30.74^{o} with the orientation of (1 1 1) and (2 0 0) planes. Two small peaks located at 44.04^{o} and 52.16^{o} to the (2 2 0) and (3 1 1) planes respectively can also be observed [13]. Figure 2 (b) shows the recorded XRD pattern of ZnS thin film deposited on glass substrate. The diffraction peaks at 27.24^{o}, 28.83^{o} and 52.39^{o} were assigned to the (1 1 0), (0 0 2) and (1 0 3) planes of the hexagonal structure [14, 23]. In this XRD pattern the peaks are wider, which indicates that the films were basically amorphous or nanocrystalline [23]. Figure 2(c) shows the XRD pattern of the $Cd_{1-x}Zn_xS$ thin films and all the peaks can be indexed to the hexagonal structure of $Cd_{7.23}Zn_{2.77}S_{10}$, which are close to standard JCPDS card No. 40-0836. The prominent 2θ values in the XRD pattern are 25.52^{o}, 27.10^{o}, 28.79^{o}, 44.87^{o} and 52.27^{o} corresponding to related planes (1 0 0), (0 0 2), (1 0 1), (1 1 0) and (2 0 0) respectively [24].The particle size can be calculated from Debye-Scherrer formula (equation 1),

Where D is the crystallite size, λ is the X-ray wavelength, β is the full width at half maximum (FWHM) and A is a constant. CZTS thin film's average particle size was calculated using equation 1 and it was found to be 18nm [18]. ZnO thin film's crystallite size was calculated to be

20nm [22]. Finally, the CdS, ZnS and $Cd_{7.23}Zn_{2.77}S_{10}$ thin films' particle size are 9nm, 13nm and14 nm respectively [13, 14, 24]. The structural parameters of CdS, ZnS and $Cd_{7.23}Zn_{2.77}S_{10}$ thin films shown in table 2.

3.2 Morphological properties

The surface morphology of the films is of great importance and can be determinant for their uniformity and indicative for the structures of the particles are formed. Figure 3(a) and (b) show the FESEM images of CZTS thin film deposited on FTO glass substrate at different magnifications. The grains of the films of the absorber layer are larger and denser after sulfurization at 550^{o}C which is very useful for highly efficient solar cells [18]. Figure 3(c) and (d) show the FESEM images of ZnO thin film at different resolution 10 μm and 5 μm respectively. Small agglomerated grains are clearly seen on the film's surface on the glass substrate [22]. Figure 4(a) and (b) show that the CdS thin film has porous and leaf like structure [25]. Figure 4(c) and (d) show that the ZnS thin film has porous and uniform flower-like morphology throughout the entire layer deposited on the glass substrate, which is even more distinctive at high resolution (5 μm) [26]. The FESEM images of $Cd_{7.23}Zn_{2.77}S_{10}$ thin film shown in Figure 4(e) and (f) are displaying uniform and petals or rod-like morphology. Moreover, the grains are well organized on the surface of the glass substrate. The $Cd_{7.23}Zn_{2.77}S_{10}$ thin film is demonstrating the strong possibility of alloy formation between ZnS and CdS materials. All the FESEM images confirmed that the nanostructured CdS, ZnS and $Cd_{7.23}Zn_{2.77}S_{10}$ thin films have a uniform morphology which is useful for solar cell applications [24-26].

3.3 Optical properties

Figure 5(a) and (b) show the $(\alpha h\nu)^2$ against the photon energy hν (inset graphs) derived from the absorption spectra of CZTS and ZnO thin film respectively. Figure 5(a) shows the absorption spectra of CZTS thin film in the visible region and a lower value for the band gap than the one anticipated occurred (1.48eV) due to excess of sulfur. A shift of the absorption edge of the absorption spectrum towards higher wavelengths, due to the sulfurization effect, increases the absorption and decreases the band gap which is good for solar cell applications [27]. Figure 5(b) shows the absorption of the ZnO thin film deposited on glass substrate by CBD method. The spectrum confirms that the ZnO thin film has low absorption in the visible region and the band gap was found to be 3.20eV [28]. Figure 6(a) shows the CdS thin film absorption spectrum which has shifted from 508 nm wavelength. From the absorption plot of CdS thin film its band gap was calculated to be 2.44eV [13]. Figure 6(b) shows the ZnS thin film absorption spectrum between the wavelength ranges from 300 nm to 900 nm. The absorption spectrum is shifted to lower wavelengths in the UV region and the band gap was calculated to be 3.72eV [14]. The optical absorption properties and the band gap of $Cd_{7.23}Zn_{2.77}S_{10}$ thin film deposited on glass substrate by CBD method are displayed in Figure 6 (c). The curve indicates direct transition and the broad band gap of $Cd_{7.23}Zn_{2.77}S_{10}$ thin film which was calculated to be 2.52eV [29].

The optical band gap value was calculated from Tauc formula (equation 2) given bellow,

$$\alpha = \frac{B(h\nu - Eg)^n}{h\nu} \text{.....(2)}$$

where B is a constant, hν is the photon energy, E_g is the optical gap and α the absorption coefficient. The CdS, ZnS and $Cd_{7.23}Zn_{2.77}S_{10}$ thin films band gap values were calculated by equation 2 to be 2.44eV, 3.72eV and 2.52eV respectively. The wide absorption spectrum and the

suitable band gap of $Cd_{7.23}Zn_{2.77}S_{10}$ thin film qualify it to be useful as a buffer layer for solar cells [29].

3.4 Photovoltaic properties

The solar cells' characteristics of the FTO/ZnO/CdS/CZTS/Ag heterojunction solar cell, with active area of 1x1 cm^2, were studied under dark and illumination (100 mW/cm^2) and the obtained electrical parameters were compared against the ones of the FTO/ZnO/ZnS/CZTS/Ag and FTO/ZnO/$Cd_{7.23}Zn_{2.77}S_{10}$/CZTS/Ag thin films' solar cells. Figure 7(a), (b) and (c) represent the current density−voltage characteristic curves under dark and illuminating conditions of the FTO/ZnO/CdS/CZTS/Ag, FTO/ZnO/ZnS/CZTS/Ag and FTO/ZnO/$Cd_{7.23}Zn_{2.77}S_{10}$/CZTS/Ag heterojunction solar cells respectively. The power conversion efficiency is calculated using the following formula (equation 3) [30]

$$\eta(\%) = \frac{P_{max}}{P_{in}} \times 100 \text{.....(3)}$$

where η is the overall efficiency of the solar cell, P_{max} is the maximum output power obtained and P_{in} is the input light power applied. Power conversion efficiency is found to increase from 0.76% to 1.24% due to the surface effect of the different buffer layers [11]. The solar cell efficiency depends on the crystallinity, the surface morphology and the interface of the p-n junction. From the FESEM images, we concluded that the particles of the $Cd_{7.23}Zn_{2.77}S_{10}$ thin film have petals or rod−like morphology which is good for solar cells. The ZnS and CdS thin films have flower and leaf−like morphology with uniform and porous structure, whereas $Cd_{7.23}Zn_{2.77}S_{10}$ thin film is more compact with a rod−like surface which can enhance the current [31]. Figure 8 shows a schematic diagram of the thin film heterojunction solar cells with the

different CdS, ZnS and CdZnS buffer layers. The surface morphology of the thin films, with limited grain boundaries, is very important to enhance the efficiency of the solar cells [31]. Under illumination the FTO/ZnO/ZnS/CZTS/Ag heterojunction solar cells' efficiency is 0.76% which is lower than the corresponding efficiency of the FTO/ZnO/CdS/CZTS/Ag cells, which was calculated to be 1.00%. The surface morphology of the buffer layer of the FTO/ZnO/$Cd_{7.23}Zn_{2.77}S_{10}$/CZTS/Ag solar cells has improved the cells' efficiency which was calculated to be 1.24%. The larger open circuit voltage of the FTO/ZnO/$Cd_{7.23}Zn_{2.77}S_{10}$/CZTS/Ag solar cells has also contributed to their higher efficiency [32, 33]. Similar behavior among three samples was observed in J-V curves under dark with which means similar electron leakage properties in all cells.

4. Conclusions

CZTS, ZnO, CdS, ZnS and $Cd_{7.23}Zn_{2.77}S_{10}$ thin films where synthesized by simple chemical methods in order to be used for fabricating heterojunction solar cells. Firstly, the structural, morphological and optical properties of the CZTS, ZnO, CdS, ZnS and $Cd_{7.23}Zn_{2.77}S_{10}$ thin films deposited on glass substrates were studied. Kesterite structure of CZTS thin film has confirmed by XRD and Raman spectroscopy. The nanostructured properties of the CdS, ZnS and $Cd_{7.23}Zn_{2.77}S_{10}$ buffer layers were confirmed by the FESEM images and the XRD spectroscopy. Flower, leaf and petals or rod−like surface morphologies of the CdS, ZnS and $Cd_{7.23}Zn_{2.77}S_{10}$ thin buffer layers have enhanced the current of the heterojunction solar cells. The absorption spectra and the band gap of the absorber layer and the buffer layers were determined from the optical measurements. CZTS has a direct band gap and an optimum absorption in the visible range which is good for the absorber layer. ZnS, CdS and $Cd_{7.23}Zn_{2.77}S_{10}$ thin films are used as wide band gap buffer layers in heterojunction solar cells and their band gaps were calculated to be

3.72eV, 2.44eV and 2.52eV respectively. The power conversion efficiency of the FTO/ZnO/ZnS/CZTS/Ag and FTO/ZnO/CdS/CZTS/Ag solar cells was calculated 0.76% and 1.00% respectively, while the FTO/ZnO/$Cd_{7.23}Zn_{2.77}S_{10}$/CZTS/Ag solar cells exhibited the highest efficiency which was estimated to be 1.24%.

Acknowledgement

The author is thankful to The Head, Department of Physics and Department of Nanotechnology, Dr. Babasaheb Ambedkar Marathwada University, Aurangabad for providing laboratory facility for carrying out the research work. Sandip Mahajan is also thankful Erasmus Mundus Lot 13 project 2013-2540/001-001-EM2 for providing financial support and research facility.

References

[1] Xiangbo Song, Xu Ji, Ming Li, Weidong Lin, Xi Luo, H. Zhang, A Review on Development Prospect of CZTS Based Thin Film Solar Cells, Int. J. Photoenergy, 2014 (2014) 613173-613184.

[2] N. Ali, A. Hussain, R. Ahmed, M.K. Wang, C. Zhao, B.U. Haq, Y.Q. Fu, Advances in nanostructured thin film materials for solar cell applications, Renewable Sustainable Energy Rev., 59 (2016) 726-737.

[3] H. Katagiri, K. Jimbo, W.S. Maw, K. Oishi, M. Yamazaki, H. Araki, A. Takeuchi, Development of CZTS-based thin film solar cells, Thin Solid Films, 517 (2009) 2455-2460.

[4] O.P. Singh, R. Parmar, K.S. Gour, M.K. Dalai, J. Tawale, S.P. Singh, V.N. Singh, Synthesis and characterization of petal type CZTS by stacked layer reactive sputtering, Superlattices Microstruct., 88 (2015) 281-286.

[5] M.A. Green, K. Emery, Y. Hishikawa, W. Warta, E.D. Dunlop, Solar cell efficiency tables (version 46), Prog. Photovoltaics Res. Appl., 23 (2015) 805-812.

[6] W. Wang, M.T. Winkler, O. Gunawan, T. Gokmen, T.K. Todorov, Y. Zhu, D.B. Mitzi, Device Characteristics of CZTSSe Thin-Film Solar Cells with 12.6% Efficiency, Adv.Eng. Mater., 4 (2014) 1301465-n/a.

[7] D. Hariskos, S. Spiering, M. Powalla, Buffer layers in Cu(In,Ga)Se_2 solar cells and modules, Thin Solid Films, 480–481 (2005) 99-109.

[8] F. Aslan, A. Tumbul, Non-vacuum processed Cu_2ZnSnS_4 thin films: Influence of copper precursor on structural, optical and morphological properties, J. Alloys Compd., 612 (2014) 1-4.

[9] A.V. Moholkar, S.S. Shinde, G.L. Agawane, S.H. Jo, K.Y. Rajpure, P.S. Patil, C.H. Bhosale, J.H. Kim, Studies of compositional dependent CZTS thin film solar cells by pulsed laser

deposition technique: An attempt to improve the efficiency, J. Alloys Compd., 544 (2012) 145-151.

[10] K. Patel, D.V. Shah, V. Kheraj, Influence of deposition parameters and annealing on Cu_2ZnSnS_4 thin films grown by SILAR, J. Alloys Compd., 622 (2015) 942-947.

[11] M. Nguyen, K. Ernits, K.F. Tai, C.F. Ng, S.S. Pramana, W.A. Sasangka, S.K. Batabyal, T. Holopainen, D. Meissner, A. Neisser, L. H.Wong, ZnS buffer layer for $Cu_2ZnSn(SSe)_4$ monograin layer solar cell, Sol. Energy, 111 (2015) 344-349.

[12] M. Dhankhar, O. Pal Singh, V.N. Singh, Physical principles of losses in thin film solar cells and efficiency enhancement methods, Renewable Sustainable Energy Rev., 40 (2014) 214-223.

[13] W.G.C. Kumarage, R.P. Wijesundera, V.A. Seneviratne, C.P. Jayalath, B.S. Dassanayake, Tunable optoelectronic properties of CBD-CdS thin films via bath temperature alterations, J. Phys. D: Appl. Phys., 49 (2016) 095109.

[14] R.K. Choubey, K. Sunil, C.W. Lan, Shallow chemical bath deposition of ZnS buffer layer for environmentally benign solar cell devices, Adv. Nat. Sci. Nanosci. Nanotech., 5 (2014) 025015.

[15] Guozhi Jia, Na Wang, Lei Gong, X. Fei, Growth characterization of CdZnS thin film prepared by chemical bath deposition, Chalcogenide Letters, 6 (2009) 463 – 467.

[16] S.B. Jambure, S.J. Patil, A.R. Deshpande, C.D. Lokhande, A comparative study of physico-chemical properties of CBD and SILAR grown ZnO thin films, Mater. Res. Bull., 49 (2014) 420-425.

[17] R.S. Mane, C.D. Lokhande, Chemical deposition method for metal chalcogenide thin films, Mater. Chem. Phys., 65 (2000) 1-31.

[18] S. Ma, J. Sui, L. Cao, Y. Li, H. Dong, Q. Zhang, L. Dong, Synthesis of Cu_2ZnSnS_4 thin film through chemical successive ionic layer adsorption and reactions, Appl. Surf. Sci., 349 (2015) 430-436.

[19] H.R. Jung, S.W. Shin, K.V. Gurav, M.P. Suryawanshi, C.W. Hong, H.S. Yang, J.Y. Lee, J.H. Moon, J.H. Kim, Phase evolution of Cu_2ZnSnS_4 (CZTS) kesterite thin films during the sulfurization process, Ceram. Int., 41 (2015) 13006-13011.

[20] S.A. Vanalakar, S.W. Shin, G.L. Agawane, M.P. Suryawanshi, K.V. Gurav, P.S. Patil, J.H. Kim, Effect of post-annealing atmosphere on the grain-size and surface morphological properties of pulsed laser deposited CZTS thin films, Ceram. Int., 40 (2014) 15097-15103.

[21] D. Seo, J. Na, C. Kim, C. Jeong, S. Lim, Improvement of Cu_2ZnSnS_4 thin film properties by a modified sulfurization process, Thin Solid Films, 591, Part B (2015) 289-294.

[22] S. M. Pawar, K. V. Gurav, S. W. Shin, D. S. Choi, I.K.Kim, C. D. Lokhande, J. I. Rhee, J.H. Kim, Effect of Bath Temperature on the Properties of Nanocrystalline ZnO Thin Films, J. Nanosci. Nanotechnol., 10 (2010) 3412–3415.

[23] T. Liu, H. Ke, H. Zhang, S. Duo, Q. Sun, X. Fei, G. Zhou, H. Liu, L. Fan, Effect of four different zinc salts and annealing treatment on growth, structural, mechanical and optical properties of nanocrystalline ZnS thin films by chemical bath deposition, Mater. Sci. Semicond. Process., 26 (2014) 301-311.

[24] Y.C. Zhang, W.W. Chen, X.Y. Hu, Controllable Synthesis and Optical Properties of Zn-Doped CdS Nanorods from Single-Source Molecular Precursors, Cryst. Growth Des., 7 (2007) 580-586.

[25] A. Kariper, E. Guneri, F. Gode, C. Gumus, Effect of pH on the physical properties of CdS thin films deposited by CBD, Chalcogenide Letters, 9 (2012) 27 – 40.

[26] J. Liu, A. Wei, Y. Zhao, Effect of different complexing agents on the properties of chemical-bath-deposited ZnS thin films, J. Alloys Compd., 588 (2014) 228-234.

[27] C. Malerba, F. Biccari, C.L. Azanza Ricardo, M. Valentini, R. Chierchia, M. Müller, A. Santoni, E. Esposito, P. Mangiapane, P. Scardi, A. Mittiga, CZTS stoichiometry effects on the band gap energy, J. Alloys Compd., 582 (2014) 528-534.

[28] S.K. Shaikh, S.I. Inamdar, V.V. Ganbavle, K.Y. Rajpure, Chemical bath deposited ZnO thin film based UV photoconductive detector, J. Alloys Compd., 664 (2016) 242-249.

[29] I. Carreon-Moncada, L.A. Gonzalez, M.I. Pech-Canul, R. Ramirez-Bon, Cd1 − xZnxS thin films with low Zn content obtained by an ammonia-free chemical bath deposition process, Thin Solid Films, 548 (2013) 270-274.

[30] Y. Sato, K. Yamagishi, M. Yamashita, Multilayer Structure Photovoltaic Cells, Opt. Rev., 12 (2005) 324-327.

[31] L. Dongwook, Y. Kijung, Solution-processed Cu_2ZnSnS_4 superstrate solar cell using vertically aligned ZnO nanorods, Nanotechnology, 25 (2014) 065401.

[32] C. Yan, F. Liu, K. Sun, N. Song, J.A. Stride, F. Zhou, X. Hao, M. Green, Boosting the efficiency of pure sulfide CZTS solar cells using the In/Cd-based hybrid buffers, Sol. Energy Mater. Sol. Cells, 144 (2016) 700-706.

[33] K. Sun, C. Yan, F. Liu, J. Huang, F. Zhou, J.A. Stride, M. Green, X. Hao, Over 9% Efficient Kesterite Cu_2ZnSnS_4 Solar Cell Fabricated by Using $Zn_{1-x}Cd_xS$ Buffer Layer, Adv. Eng. Mater., 6 (2016) 1600046-n/a.

Figure Captions

Fig. 1: (a) & **(b)** XRD pattern and Raman spectrum graph of CZTS thin film and **(c)** XRD pattern of ZnO thin film.

Fig. 2: (a), (b) & **(c)** represents XRD pattern of CdS, ZnS and $Cd_{7.23}Zn_{2.77}S_{10}$ thin films respectively.

Fig. 3: FE-SEM images of **(a-b)** CZTS thin film and **(c-d)** ZnO thin film respectively.

Fig. 4: FE-SEM images of **(a-b)** CdS, **(c-d)** ZnS and **(e-f)** $Cd_{7.23}Zn_{2.77}S_{10}$ thin films respectively.

Fig. 5: Shows absorption spectra and **inset** shows the band gap of **(a)** CZTS thin film and **(b)** ZnO thin films respectively.

Fig. 6: Shows absorption spectra and **inset** shows the band gap of **(a)** CdS; **(b)** ZnS and **(c)** $Cd_{7.23}Zn_{2.77}S_{10}$ thin films respectively.

Fig. 7: J-V characteristics curve obtained from **(a)** FTO/ZnO/CdS/CZTS/Ag, **(b)** FTO/ZnO/ZnS/CZTS/Ag and **(c)** FTO/ZnO/$Cd_{7.23}Zn_{2.77}S_{10}$/CZTS/Ag heterojunction solar cells under dark and under illumination of Xenon 100mW/cm^2 light source.

Fig. 8: Schematic representation of probable heterojunction solar cells and surface morphology of CdS, ZnS and $Cd_{7.23}Zn_{2.77}S_{10}$ buffer layers respectively.

Table 1

Structural parameters of CZTS and ZnO thin films.

Sr. No.	Method	2θ (deg.)	(hkl) planes	FWHM (β) (10^{-3} radian)	Crystallite size (D) (nm)
1	CZTS	28.14	(1 1 2)	0.7594	18.8
		47.49	(2 2 0)	1.0352	14.6
		56.52	(3 1 2)	0.8311	18.9
		Average value			17.04
2	ZnO	31.72	(1 0 0)	0.7313	19.7
		34.36	(0 0 2)	0.6203	23.3
		36.21	(1 0 1)	0.7081	20.5
		47.21	(1 0 2)	0.7515	20.1
		62.75	(1 0 3)	0.9265	17.5
		Average value			20.26

Table 2

Structural parameters of CdS, ZnS and $Cd_{7.23}Zn_{2.77}S_{10}$ thin films

Sr. No.	Method	2θ (deg.)	hkl planes	FWHM(β) (10^{-3} radian)	Crystallite size (D) (nm)
1	CdS	26.69	(1 1 1)	0.1394	10.2
		29.59	(2 0 0)	1.2707	11.2
		44.01	(2 2 0)	1.7174	08.7
		52.01	(3 1 1)	2.6043	05.9
		Average value			9.03
2	ZnS	27.02	(1 0 0)	1.1156	12.7
		28.9	(0 0 2)	1.5119	09.4
		52.01	(1 0 3)	0.9399	16.4
		Average value			12.8
3	$Cd_{7.23}Zn_{2.77}S_{10}$	25.58	(1 0 0)	1.2464	11.4
		27	(0 0 2)	0.8551	16.6
		28.61	(1 0 1)	0.6402	22.3
		44.09	(1 1 0)	0.2258	06.6
		51.35	(2 0 0)	1.0969	14.0
		Average value			14.21

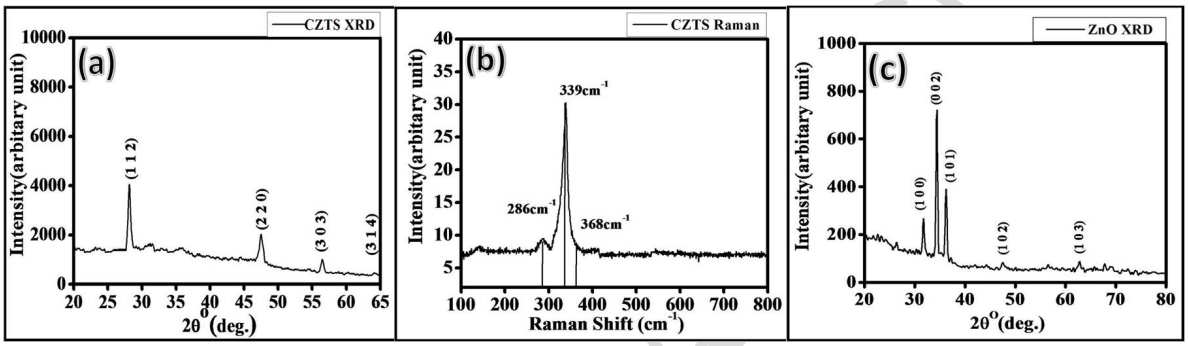

Fig. 1: Mahajan et. al.

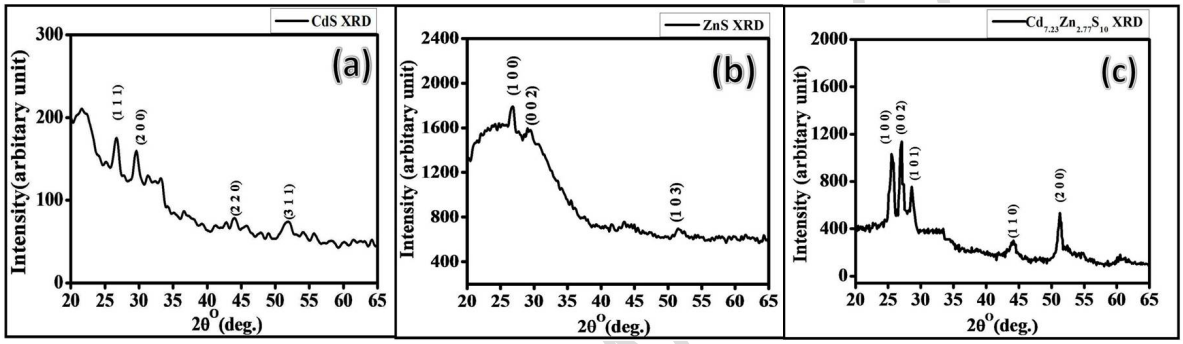

Fig. 2: Mahajan et. al.

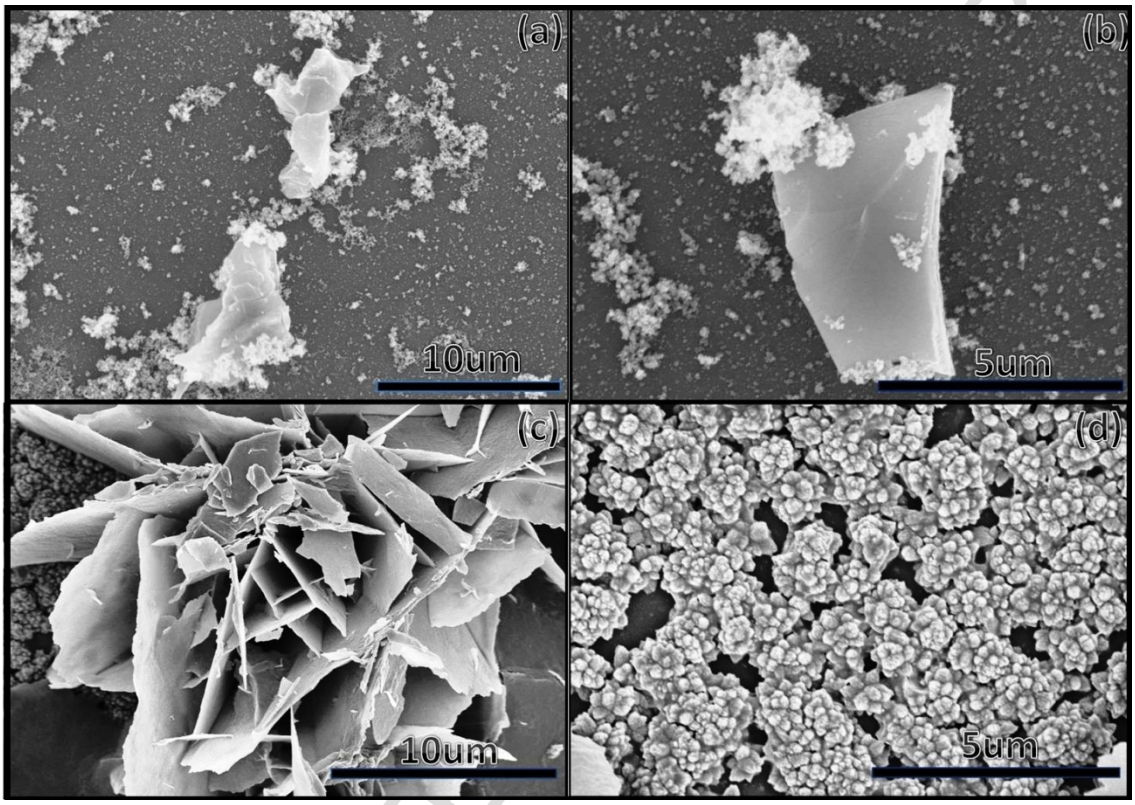

Fig. 3: Mahajan et. al.

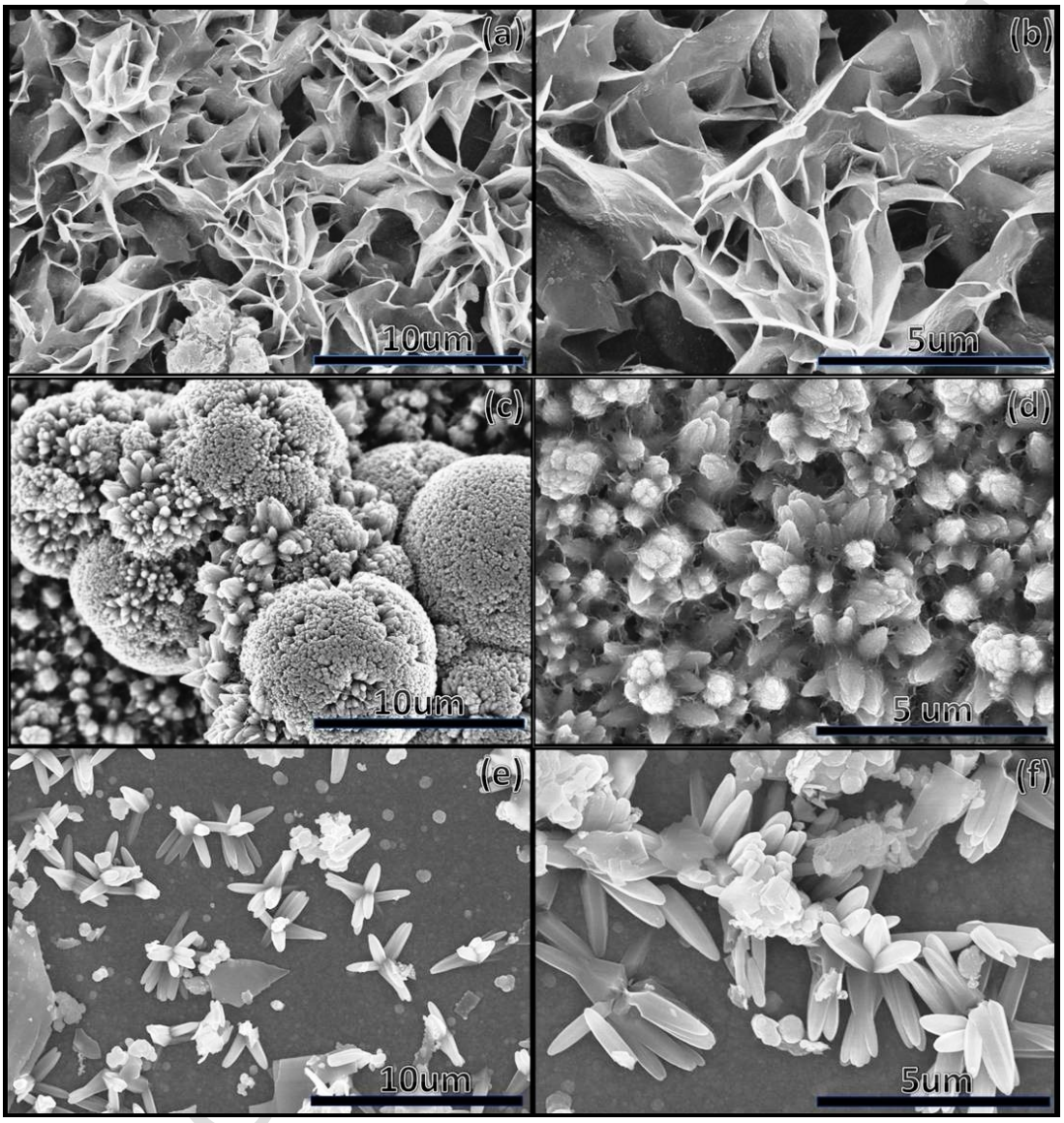

Fig. 4: Mahajan et. al.

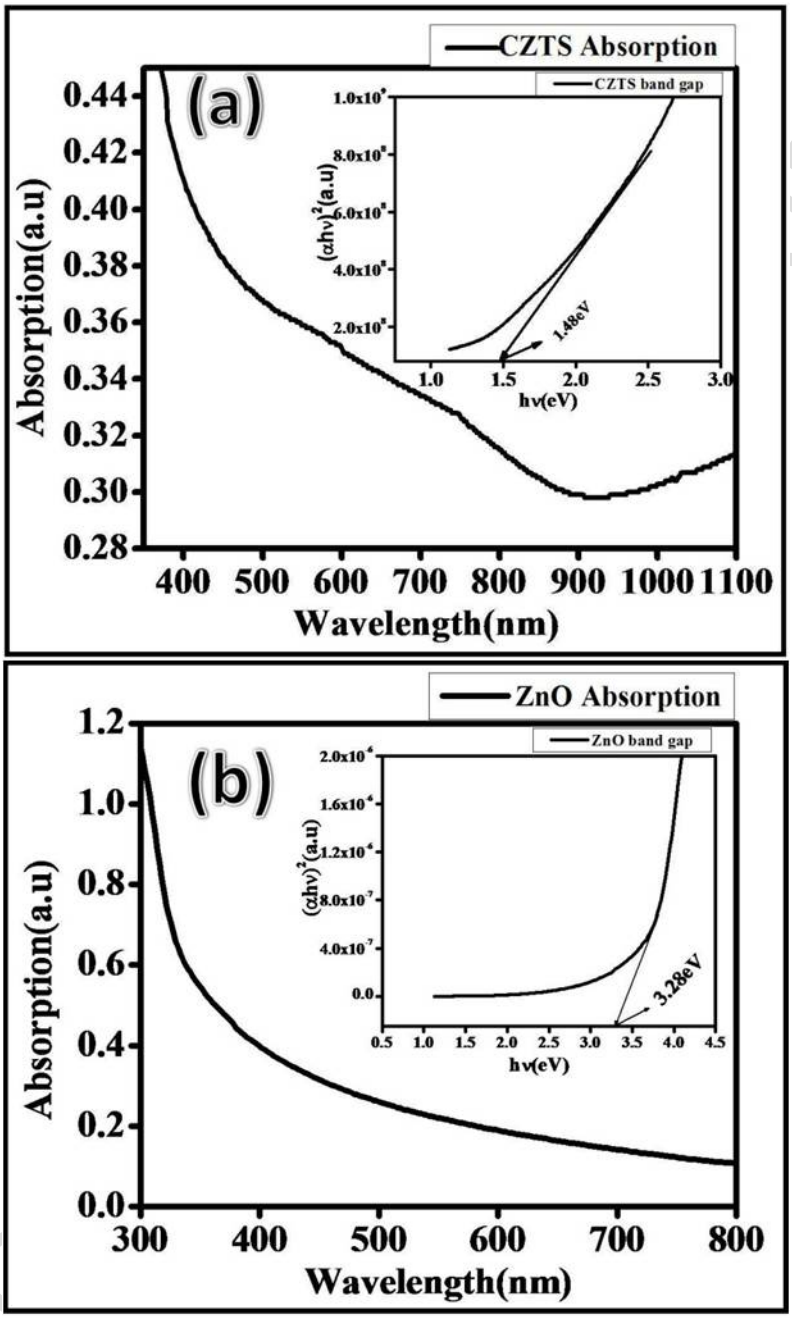

Fig. 5: Mahajan et. al.

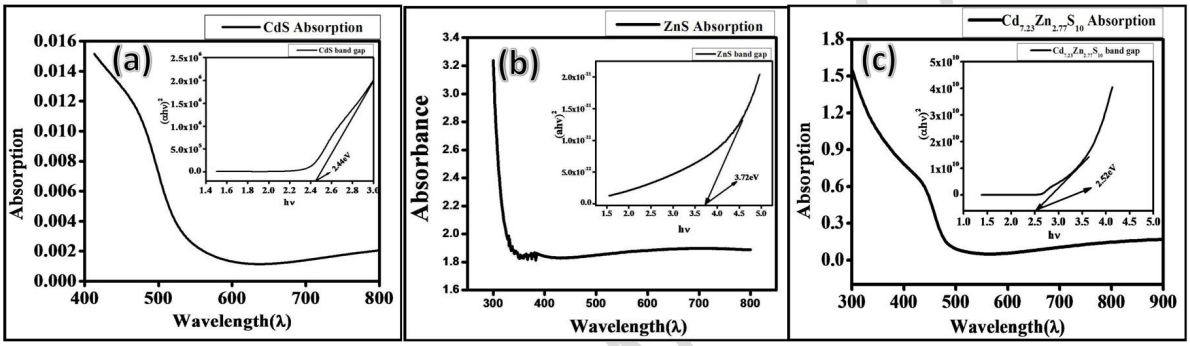

Fig. 6: Mahajan et. al.

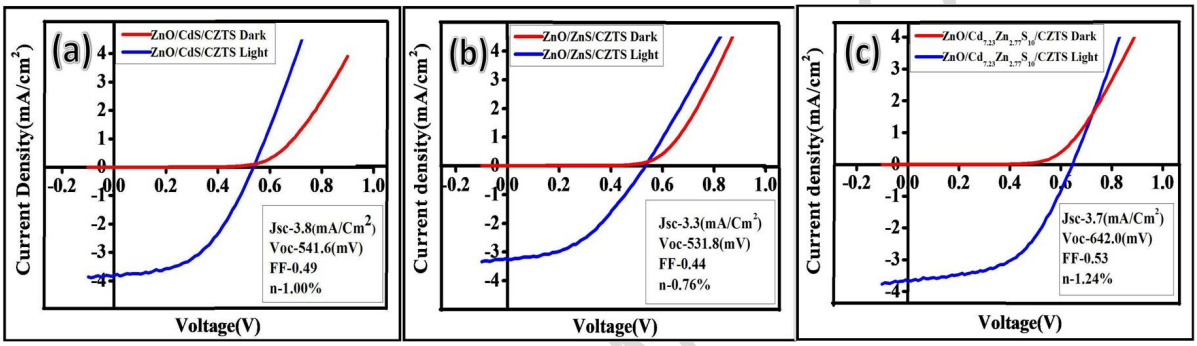

Fig. 7: Mahajan et. al.

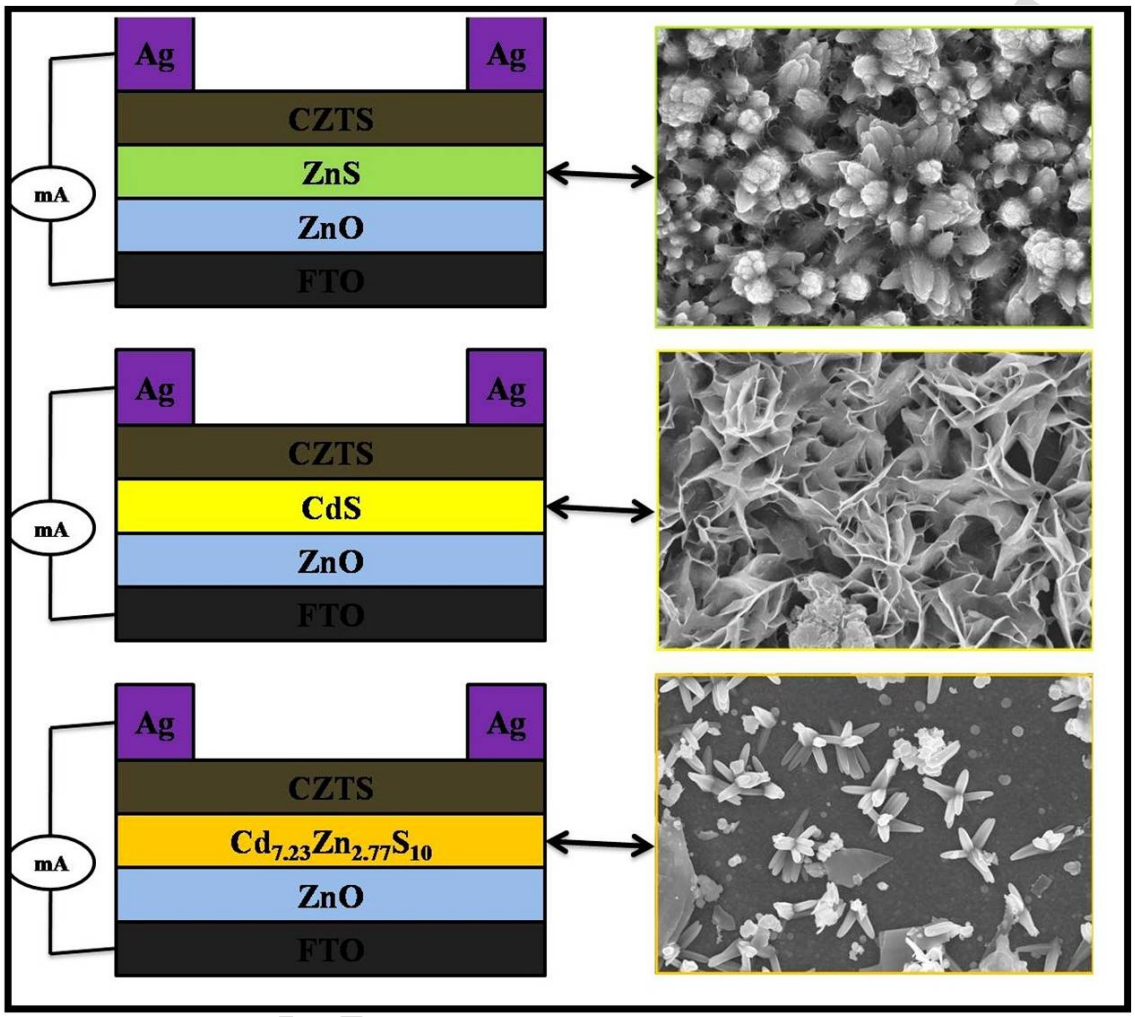

Fig. 8: Mahajan et. al.